

# Tracking Detectors for CLAS12

Mac Mestayer and Daniel S. Carman and YOUR NAME HERE

January 9, 2007

## 1 Overview of CLAS12 Physics

The CLAS detector in Hall B is being upgraded to take advantage of the increase of the CEBAF beam energy from 6 to 12 GeV, thus the new name, CLAS12. There are several broad areas of physics enquiry that drive these changes: spectroscopic studies of excited baryons, investigations of the influence of nuclear matter on propagating quarks, studies of polarized and unpolarized quark distributions, and a comprehensive measurement of generalized parton distributions (GPDs). The reactions of interest are electroproduction of exclusive and semi-inclusive final states. The cross sections for these processes are small, necessitating the use of high-luminosity experiments. A variety of simulated experiments rely on luminosities of  $10^{35} \text{ cm}^{-2}\text{s}^{-1}$  to achieve the desired statistical accuracy in runs of a few months duration. The deep exclusive reactions in which an electron scattering at moderate to high values of  $Q^2$  results in a meson-baryon final state, provides the most stringent test of the CLAS12 tracking system. A final state of a few high-momentum, forward-going particles (the electron as well as one or more mesons), combined with a moderate-momentum baryon emitted at large angles, is the typical event type on which the specifications of the tracking system are based.

In broad strokes, the tracking system must measure forward-going particles down to laboratory angles as small as  $5^\circ$  in order to cover the kinematically interesting regions of the experiment. In addition, a fractional momentum resolution of 1% for momenta up to about 5 GeV is necessary in order to positively identify a missing particle in these exclusive reactions. Because the relevant cross sections are small, the tracking system must have high efficiency and low fake rates even at a luminosity of  $10^{35} \text{ cm}^{-2}\text{s}^{-1}$ .

Finally, good vertex resolution will allow detection of secondary decay vertex and serve as a good marker for strangeness production. Because  $c\tau$ 's of most strange particles are in the range of a few centimeter and because typical momenta range from 0.5 to 5 GeV/c, a vertex resolution of 1 cm is sufficient. With typical opening angles of  $12^\circ$  (for example, the symmetric decay of a  $\Lambda$  with a momentum of 2 GeV/c) a 1 cm vertex resolution translates into a requirement for a 1 mm impact parameter resolution (perpendicular to the track).

A tracking system capable of achieving these standards was described in the PCDR [1] and quantitatively parameterized in a “fast” Monte Carlo [2] program.

A number of CLAS collaborators used the model of the detector as described in the FASTMC in proposals presented at the latest JLab PAC [3].

## 2 Overview of the CLAS12 Detector

As noted in the previous section, the new detector is being designed to operate at a luminosity of  $10^{35} \text{ cm}^{-2}\text{s}^{-1}$ . This higher luminosity goal (the present CLAS detector operates at a maximum luminosity of  $10^{34} \text{ cm}^{-2}\text{s}^{-1}$ ) necessitates the use of a solenoidal magnet and conical absorber to shield the detector from Møller electrons. To reduce interactions between this solenoidal field and a toroidal field, and to facilitate construction and installation of new detector elements, the torus has been re-designed. It is more compact than the present torus while providing equivalent bending power for charged particles between 5 and  $45^\circ$ .

We have designed the tracking detectors with these external constraints: a central solenoid of 5 T central field value and a radius available for tracking detectors of 25 cm, a new torus with a different aspect ratio but with the same number of amp-turns as the present CLAS torus, an expected background rate consistent with a luminosity of  $10^{35} \text{ cm}^{-2}\text{s}^{-1}$  and a separation between the “forward” and “central” regions defined to be at about  $45^\circ$  degrees; specifically the forward tracking chambers are designed to cover scattering angles between  $5^\circ$  and  $45^\circ$  and the central tracker will cover  $40^\circ$  to  $135^\circ$ . Although the torus cryostat will limit the azimuthal coverage to about 50% at  $5^\circ$ , our goal is the the drift chambers’ dead areas not further intrude into the active volume; i.e. the dead areas of the drift chambers (endplates, electronics, etc.) will be located in the “shadow” of the coil as viewed from the target.

The higher beam energies available to CLAS12 mean that tracks will go more forward and have higher momentum than for the present CLAS experiments. We thus require better resolution from the forward drift chambers, mandating a smaller cell size. The other feature of higher energy, smaller cross sections, requires the use of higher intensity beams. The resultant higher backgrounds can also be mitigated by the smaller cell sizes.

The goal is to achieve a fractional momentum resolution of 1% at a track momentum of 5 GeV. Because on average only about 10% of the total charged particle momenta is measured in the central tracker, its design value for the fractional momentum resolution at a momentum of 1 GeV is 10%.

We have studied two options for central tracks: 8 layers of silicon strips with alternating plus and minus stereo angle strips being one, and 4 layers of silicon followed by an 8-layer micromegas detector being the other. For forward tracks we have a conceptual design based upon 6 layers of silicon with alternating plus/minus stereo angle strips followed by three regions of drift chambers with the wires of each chamber arranged in two 6-layer “superlayers” with alternating plus/minus stereo angles.

A side-view of the proposed CLAS12 detector (cut through the beamline) is shown in Fig. 1. A solenoidal magnet contains the target, the central silicon

vertex tracker (SVT), and the central time-of-flight system (CTOF), as well as the Møller absorber. Charged particles with emission angles greater than  $40^\circ$  follow helical paths through the 8 layers of the SVT, which are arranged into four  $U - V$  modules with “ $U$ ” and “ $V$ ” referring to strip orientations of  $\pm 1.5^\circ$ , respectively. The time resolution of the CTOF ( $\sim 200$  ps) will enable particle identification of the charged tracks, as well as allowing a very efficient rejection of out-of-time accidentals.

Forward-going tracks (with angles less than  $45^\circ$ ) pass through the forward vertex tracker (FVT) which is arranged into three  $U - V$  modules with the “ $U$ ” and “ $V$ ” strips oriented at  $\pm 1.5^\circ$  angles. Following the FVT is a high-threshold Čerenkov counter (HTCC), a threshold Čerenkov counter filled with atmospheric  $\text{CO}_2$  gas, designed for electron identification. It will effectively reject other charged particles, up to the momentum threshold for pions ( $\sim 6$  GeV). Following the HTCC is the toroidal magnet which, besides providing the magnetic field for momentum analysis, supports three regions of drift chambers (denoted Regions 1, 2, and 3) for charged track detection. Regions 1 and 3 are attached to the front and rear faces of the toroid, while Region 2 is located between the torus coils.

Following the torus-drift chamber assembly is the forward detector, consisting of a low-threshold Čerenkov counter (LTCC) for charged hadron identification, the main time-of-flight (TOF) system, and the pre-shower calorimeter (PCAL) and main electromagnetic calorimeter (EC). The TOF is used to define the main event start time and to enhance charged hadron identification, while the PCAL and EC are used for electron and photon detection.

Figure 1: A side-view of the CLAS12 detector showing the different detector subsystems, and highlighting the central and forward vertex trackers and drift chambers.

### 3 Event Characteristics

As discussed in the physics overview, the CLAS12 detector is designed to detect semi-inclusive and exclusive events with a modest (up to 4 or 5) number of outgoing hadrons. In addition to the electron and hadrons associated with the event of interest, the detected event will contain both electromagnetic and hadronic “accidentals”. Because the physics goal is to run at beam-target luminosities of  $10^{35} \text{ cm}^{-2}\text{s}^{-1}$  or higher, we have extensively simulated the expected accidental particle flux associated with these luminosities.

Using a modified version of the EGS program, we simulated the total hadronic and electromagnetic particle fluxes generated when an electron beam is incident upon a liquid-hydrogen target with a luminosity of  $10^{35} \text{ cm}^{-2}\text{s}^{-1}$ . We calculated the total flux through a measurement layer during its active (measurement) time and multiplied by the probability of the particle interacting in that layer and divided by the number of cells in the layer to get an estimate of the fractional occupancy of that layer due to background. Our experience with the present CLAS detector is that track-finding is highly efficient if the accidental occupancy is less than 4-5% [4]. In Table 1 we show the number of cells, the detector live-time, the flux per layer, the interacting flux per layer, and finally the expected accidental occupancy per layer for a luminosity of  $10^{35} \text{ cm}^{-2}\text{s}^{-1}$  and for our “standard” solenoidal Møller shield.

| Layer          | svt1 | svt8 | fsvt1 | fsvt6 | dc1 | dc36 |
|----------------|------|------|-------|-------|-----|------|
| gammas/sec     |      |      |       |       |     |      |
| electrons/sec  |      |      |       |       |     |      |
| hadrons/sec    |      |      |       |       |     |      |
| acc. occupancy |      |      |       |       |     |      |

Table 1: Average event characteristics for CLAS12.

In Fig. 2 we show a single simulated event in the proposed CLAS12 detector.

### 4 Tracking Requirements and Design Overview

To summarize, we are designing the CLAS12 tracking system with the requirements shown in Table 2.

Forward tracks (angles between  $5^\circ$  and  $40^\circ$ ) will be momentum-analyzed by passing through the magnetic field of the torus. Such tracks will first pass through six layers of a forward silicon vertex tracker (FSVT); a silicon strip tracker with a strip pitch of  $300 \mu\text{m}$  arranged with alternating  $U - V$  stereo layers with a stereo angle of  $\pm 15^\circ$  located about 20 cm from the target. These tracks will then traverse the low-threshold Čerenkov counter (LTCC) before entering the Region 1 drift chamber at a distance of 2.1 m from the target. The track continues through the magnetic field region and its trajectory is measured

Figure 2: A side-view of the **CLAS12** detector (only the tracking system is shown) displaying the hits from a simulated single event along with background hits expected at a luminosity of  $10^{35} \text{ cm}^{-2}\text{s}^{-1}$

| <b>Category</b>     | <b>Requirement</b>                     |
|---------------------|--|
| Angular coverage    | 5 - 140°                               |
| Momentum resolution | $dp = 0.05 \text{ GeV}$                |
| Angular resolution  | 1 mrad                                 |
| Min. luminosity     | $10^{35} \text{ cm}^{-2}\text{s}^{-1}$ |

Table 2: General specifications for **CLAS12** tracking.

in two more drift chambers, denoted Regions 2 and 3, respectively. The Region 2 and 3 chambers are located at 3.3 and 4.5 m from the target, respectively. The FSVT should localize hits with an estimated accuracy of about  $50 \mu\text{m}$  perpendicular to the strip direction, while the three regions of drift chambers are expected to have spatial resolutions of about  $200 \mu\text{m}$  per layer. The expected momentum resolution from such an assembly is expected to be about 1% and nearly constant as a function of momentum. The angular resolution falls rapidly with increasing momentum, but should be better than 2 mrad at a momentum of 1 GeV. See the section on expected performance for graphs of the results of these simulations.

## 5 Central Vertex Tracker

There are two options for a central tracker: an 8-layer silicon strip detector or a 4-layer silicon strip detector surrounded by an 8-layer micromegas chamber. The 8-layer silicon strip detector is the standard option. The silicon strips are laid out with a  $\pm 1.5^\circ$  stereo angle as are alternate layers in the micromegas tracker. Each design consists of concentric shells of measurement layers at successively greater radius. The  $r - \phi$  coordinate is measured by the strip coordinate in either case. The  $r - z$  coordinate is measured by a stereo angle projection. Table 3 lists the specifications for the two alternative designs. Fig. 3 highlights the central SVT.

|                        | <b>all-silicon</b> | <b>Silicon + MM</b> |
|------------------------|--------------------|---------------------|
| num. layers            | 8                  | 12                  |
| rmin:rmax              | 5.0:15.5           | 5.5:23.5            |
| num. cells per layer   | 3000               | 64 - 156            |
| assumed resolution     | 0.0028 - 0.0087 cm | 0.02 cm             |
| total thickness (r.l.) | 0.02               | 0.005               |

Table 3:

The central silicon tracker design consists of eight single-sided silicon strip detectors. Each detector plane is formed as a hexagonal shell with the silicon strips running at  $1.5^\circ$  with respect to the  $z$ -direction. This detector has good intrinsic resolution in the  $r - \phi$  coordinate. It relies on a small stereo angle to determine the  $r - z$  position of tracks. The stereo angle of the strips is equal to  $1.5^\circ$ . Table 3 lists the specifications for the central silicon tracker.

## 6 Forward Vertex Tracker

The forward silicon tracker consists of six single-sided silicon strip detector planes. Each plane is formed from six pieces, each roughly triangular in shape with strips on one plane running parallel to one of the sides of the triangle with

Figure 3: A cut-view of the central SVT looking along the beam direction. The individual sensors overlap in eight layers forming four superlayers of adjacent  $\pm 1.5^\circ$   $U - V$  strip orientations.

readout on the outer-radius side and strips from the other plane being parallel to the other side of the triangle. In this way, the strips cover the entire area of the triangular surface and always run to the “outside” where the readout electronics is located. The strips vary in length, from the longest which is adjacent to its parallel side down to a short strip opposite. See Fig. 4 for a layout of the detector and Table 4 for the detector specifications.

|                    | <b>Region 1</b> | <b>Region 2</b> | <b>Region 3</b> |
|--------------------|-----------------|-----------------|-----------------|
| dist. from target  | 10 cm           | 18 cm           | 26 cm           |
| num. $U/V$ strips  | ?               | ?               | ?               |
| stereo angle       | ?               | ?               | ?               |
| strip width        | 0.01 cm         | 0.02 cm         | 0.03 cm         |
| assumed resolution | 0.0028 cm       | 0.0058 cm       | 0.0087 cm       |

Table 4:

## 7 Drift Chambers

The overall tracking requirements (1% fractional momentum resolution at 5 GeV/c and efficient tracking at a luminosity of  $10^{35} \text{ cm}^{-2}\text{s}^{-1}$ ) are the main drivers for drift chamber design. Because the CLAS drift chamber system [4] has operated successfully for 8 years, we plan to re-use many of the design

Figure 4: A vertical cut through the forward SVT showing its arrangement into 3 superlayers of  $2 \pm 1.5^\circ$   $U - V$  stereo strips.

concepts and most of the utility infrastructure. In particular, we plan to reuse the present gas mixing and handling system, the high-voltage and low-voltage systems, the FASTBUS TDC system and the post-amplifier/multiplexer systems. The construction project thus consists of new chambers, on-board electronics and on-board jumper cables.

The required better resolution of the tracking system compared to present CLAS will be achieved by chambers with a smaller cell size and thus inherently better spatial resolution and the smaller physical size and thus more accurate placement of the chambers with respect to the magnet coils. The design of the forward chambers is very similar to the present CLAS chambers. The cell design is hexagonal and the sense wire layers are arranged in 6-layer superlayers as in the present chambers. The major difference is that the cells are approximately two thirds as big as the present chambers allowing efficient tracking at higher luminosities because the accidental occupancy from particles not associated with the event is smaller. Table 5 lists the design parameters and Fig. 5 shows a cut-view of the layer and superlayer arrangement of the wires. For the purposes of simulating track resolutions we assumed that the position resolution of the individual drift cells would be  $200 \mu\text{m}$ .

The chambers differ from the present CLAS chambers in a number of ways. Successive superlayers have their wires arranged with a plus or minus  $6^\circ$  stereo angle; the present arrangement has an axial layer and a  $6^\circ$  stereo layer. For the present CLAS detector the  $\phi$  resolution is about four times larger than the  $\theta$  resolution. Because the contribution of the  $\phi$  resolution to, for example, the missing mass resolution becomes more important for small angles, we decided that we needed to double our effective stereo angle in order to decrease the  $\phi$



Figure 5: A vertical cut through a Region 1 drift chamber showing the projection of the wires onto the chamber midplane.

resolution. Unlike the present chambers, all of the wires in one of the superlayers are strictly parallel, and in a plane perpendicular to the wire direction form perfect hexagons. This should allow a more accurate drift velocity calibration than the current design with its layer-to-layer increase in cell size.

Another departure from the present design is to design every chamber (in all three regions) to be self-supporting in order to ensure that they are easy to install and remove for maintenance. In the present CLAS, the region one chambers are all bound together into a single unit in order to maintain the wire tension without excessively thick endplates, and the region two chambers are actually mounted onto the magnet cryostat with the cryostat itself maintaining the internal wire tension. None of the present region one or two chambers can be accessed individually without a lengthy “tension-transfer” process. To avoid this, we are designing all chambers to be self-supporting like our present region three chambers. The key will be ultra-stiff endplates which obtain their stiffness by a flanged design.

A third design change is to use 30  $\mu\text{m}$  diameter sense wire rather than the more common 20  $\mu\text{m}$  wire. Our choice of wire is 30  $\mu\text{m}$  diameter, gold-plated Tungsten for the sense wires, 140  $\mu\text{m}$  diameter, gold-plated Aluminum for the field wires and 140  $\mu\text{m}$  diameter, stainless steel for the guard wires. This should make the chamber more robust to wire breakages. Higher voltages will be required to achieve the same gas gain, and the resulting higher electric field in the drift cells will result in a more nearly constant drift velocity which should be more accurate after calibration. Prototypes are being built to study possible negative side-effects of the higher voltage operation such as leakage currents on the circuit boards and/or higher rates of cathode emission from the field wire

surfaces.

The choice of gas; a 92:08 Argon: $CO_2$  mixture is a small departure from our present 90:10 mixture and should result in a higher and more constant drift velocity.

|                             | <b>Region 1</b> | <b>Region 2</b> | <b>Region 3</b> |
|-----------------------------|-----------------|-----------------|-----------------|
| dist. from target           | 2.1 m           | 3.3 m           | 4.5 m           |
| num. of superlayers         | 2               | 2               | 2               |
| layers/superlayer           | 6               | 6               | 6               |
| wires/layer                 | 112             | 112             | 112             |
| cell size                   | 0.86 cm         | 1.36 cm         | 1.88 cm         |
| assumed resolution per wire | 0.02 cm         | 0.02 cm         | 0.02 cm         |

Table 5:

## 8 Expected Detector Performance

We studied the position, angle and momentum resolution for a number of possible detector options using MOMRES. Our procedure was to produce a MOMRES input file which characterized the detector position, material thickness and estimated hit resolution for a particular track angle. We also produced a B-field file which was a tabulation of the B-field strength versus path length for a particular track angle. These, and the desired range of momenta, was the input to MOMRES. As stated in the previous section, MOMRES calculated the expected components of the resolutions due to multiple scattering and measurement resolution, respectively. We fit these outputs to the expected kinematic form (see formulas  $dp/p$ ,  $d\theta$ , and  $dx$  for the kinematic dependence). From these fits we extracted two parameters (sig1 and sig2) for each of the three terms ( $dp/p$ ,  $d\theta$ ,  $dx$ ). These six parameters abstract the output of MOMRES. In addition, we calculated the angle resolution in the non-bend plane in a manner analogous to that of MOMRES, using estimators for the effects of multiple scattering and measurement error and fitting the resulting smeared trajectory by a straight line with adjusted starting position and angle and extracting the sig1 and sig2 parameters which characterize the resolution in this out-of-bend-plane angle. Thus, eight parameters for each value of track angle fully characterize the tracking resolution for any one detector option. Fig. 6 shows the momentum,  $\theta$ ,  $\phi$ , and vertex resolutions for three detector options for tracks emitted at  $30^\circ$ .

Figure 7 shows the momentum,  $\theta$ ,  $\phi$ , and vertex resolutions for three detector options for tracks emitted at  $90^\circ$ , i.e. into the central detector.

Fig. 8 shows the reconstructed momentum for 1000 events each containing a 1 GeV track emitted at a  $60^\circ$  polar angle but at random values of azimuthal angle and with random multiple scattering. The solid (dashed) line is for events with the background expected at a luminosity of  $10^{35} \text{ cm}^{-2}\text{s}^{-1}$  ( $10^{34} \text{ cm}^{-2}\text{s}^{-1}$ ).

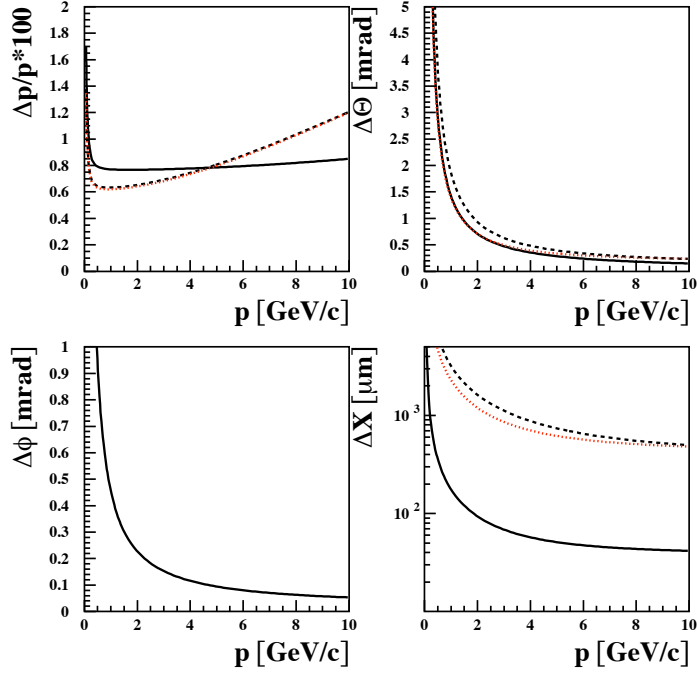


Figure 6: Resolution plotted versus particle momentum for  $30^\circ$  tracks. Sub-figures a, b, c, and d show the momentum,  $\theta$ ,  $\phi$ , and vertex resolutions, respectively. Three options are shown: solid- 3 SVT planes + CC + 3 DC planes; dashed- CC + 3 DC planes; dotted - 3 DC planes.

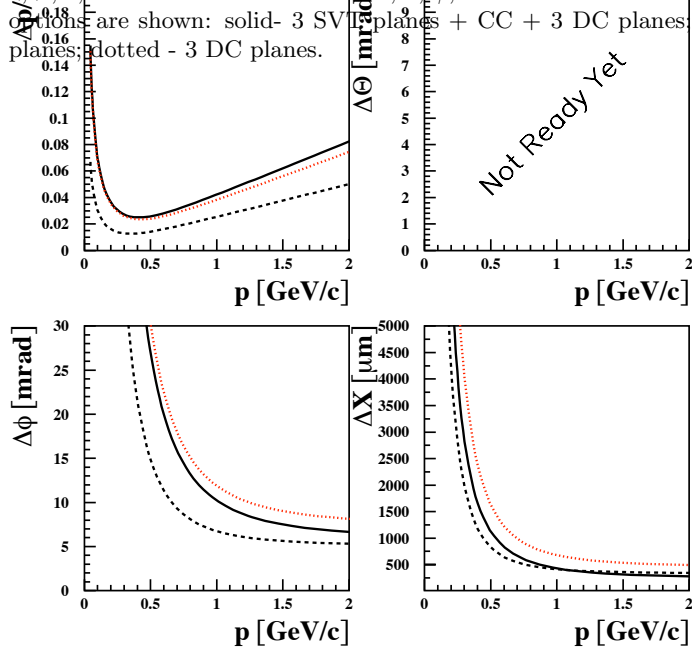


Figure 7: Resolution plotted versus particle momentum for  $90^\circ$  tracks. Sub-figures a, b, c and d show the momentum,  $\theta$ ,  $\phi$ , and vertex resolutions, respectively. Three options are shown: solid- 3 SVT planes; dashed- 16 DC-stereo planes; dotted - 8 DC-cathode pad planes.

Figure 8: A plot of reconstructed momentum for 1000 events, each containing a 1 GeV track emitted at a  $60^\circ$  polar angle but at random values of azimuthal angle and with random multiple scattering. The solid (dashed) line is for events with the background expected at a luminosity of  $10^{35} \text{ cm}^{-2}\text{s}^{-1}$  ( $10^{34} \text{ cm}^{-2}\text{s}^{-1}$ ).

## 9 Expected Physics Performance

We use a series of programs to calculate the acceptance and reconstructed physics parameters for event types of interest. The program `clasev` serves as an event generator and analysis program. Depending on the value of input flags, it generates certain types of events; that is, it produces a set of 4-momenta for the primary hadrons in the hadronic center-of-mass and allows some of them to decay into the final-state hadrons and transforms their momenta to the lab system. For each final-state track, it calls `FASTMC` to determine if the track falls within a fiducial acceptance window and to determine its final, smeared lab momentum. It then produces selected physics analysis variables such as missing mass from calculations involving the smeared momenta of those tracks which were accepted. The program `clasev` is kept under `cvs` in `cvs/12gev/fastmc/clasev`.

Figure 9 shows the expected missing mass resolution in *blah*, *blah*, *blah*. Fig. 10 is a two-dimensional plot of the acceptance for *blah*, *blah* as a function of the center-of-mass angles  $\theta$  and  $\phi$ . Note that the acceptance is non-zero over the whole kinematic range.

## References

- [1] citations to JLAB12 PCDR
- [2] location, brief description of FASTMC

Figure 9: Plot of the expected missing mass resolution for CLAS12.

Figure 10: Two dimensional plot of the acceptance as a function of the center-of-mass angles  $\theta$  and  $\phi$  for CLAS12.

[3] citations to JLAB12 pac

[4] citations to drift chamber NIM article